

The Smith Tube: Selection of Radar Chirp Waveform Bandwidth and Power Amplifier Load Impedance Using Multiple-Bandwidth Load-Pull Measurements

Matthew Fellows, Matthew Flachsbart, Jennifer Barlow, Charles Baylis, and Robert J. Marks II

Wireless and Microwave Circuits and Systems Program
Department of Electrical and Computer Engineering
Baylor University
Waco, TX, USA

Abstract—The operation of a radar system requires a trade-off between detection capabilities, power efficiency, and adjacent channel power minimization. Specifically, wide signal bandwidth is important for range detection. This paper presents how load-pull data taken for multiple linear frequency-modulated chirp waveforms with different bandwidths can be used to select the chirp waveform with the largest bandwidth possible, while meeting adjacent-channel power ratio and power-added efficiency requirements. This approach utilizes plots of adjacent-channel power ratio and power-added efficiency surfaces within a Smith tube, a three-dimensional, cylindrical extrapolation of the traditional Smith chart. A measurement example is given to illustrate the design approach. This approach will be useful in the design of range radars, and also is likely to find use in enabling real-time reconfiguration of future radars for varying spectral environments and efficiency requirements.

I. INTRODUCTION

Radar systems are being stretched to new, increasingly difficult standards of operation. The *National Broadband Plan* of 2010 in the United States mandates the release of 500 MHz of spectrum to wireless broadband applications by 2020. Radars are being required to perform their important sensing functions with less bandwidth, making range detection difficult. For example, part of the frequencies in the S-band previously allocated to radar are now shared with wireless communications, and further re-allocation of radar spectrum is imminent. Optimizing the radar transmitter design tradeoff between high power efficiency, maximum waveform bandwidth, and spectral compliance is a challenge that must be imminently addressed. It is also quite feasible that the next-generation radar transmitter will need to be flexible and reconfigurable in real-time to permit changes in operating frequency and dynamic allocation of spectrum and determination of spectral masks.

We have contributed significant literature on controlling the power efficiency and spectral output of the amplifier in

real time. Our previous work has presented the optimization of a power amplifier's load impedance for combined goals of increased power-added efficiency (PAE) while minimizing the adjacent-channel power ratio (ACPR) [1, 2]. These two works present "fast load-pull" approaches to find the Pareto optimum load impedance under conflicting linearity and efficiency requirements that can be used for the real-time optimization of radar transmitters. In the case of radar transmitters, the waveform is yet another factor in the spectral spreading of the device, and we have also published previous separate works regarding the optimization of radar chirp waveforms [3, 4]. These works, however, do not address the maximization of waveform bandwidth necessary for low-ambiguity range detection.

The present paper examines the maximization of radar waveform bandwidth while meeting predetermined requirements of power-added efficiency (PAE) and adjacent-channel power ratio (ACPR). The ability to change the bandwidth of the excitation chirp waveform adds a third design parameter (the waveform bandwidth) to the two already-present Smith chart design parameters: the real and imaginary parts of the load reflection coefficient Γ_L . To create the ability to intuitively visualize this design procedure, we have extrapolated the Smith chart to a third dimension of input waveform bandwidth B , here referred to as the *Smith tube*.

In the maximization of input bandwidth, the spectral spreading due to amplifier nonlinearities must be considered. The nonlinearity of the amplifier is a significant function of Γ_L . The dependency of nonlinearity-related spectral spreading in the case of the broadband chirp excitation can be assessed using load-pull measurements for ACPR. Other possible linearity metrics applied to slightly different problems could include error vector magnitude (EVM) and third-order intermodulation (IM3). EVM is useful in measuring the distortion in digital symbol transmission, and IM3 is most

useful in assessing fundamental device nonlinearities and predicting spreading under single- or multi-tone excitation.

The efficiency and spectral spreading of a device have both been shown to be functions of the amplifier's load impedance [5, 6]. Wu connects ACPR results for broadband signals with predictions based on third- and fifth-order intermodulation results from two-tone tests [7]. Sechi describes in his work how to find a best Pareto compromise load impedance for third order intermodulation (IM3) and efficiency [8] from pre-measured load-pull data. Our previous work shows a vector-based, real-time optimization for a Pareto optimum of PAE and ACPR under broadband signal excitation [2]. [2] presents a vector-based search algorithm that reduces the number of measurements necessary for an optimization, and is expected to find usefulness in the real-time optimization of radar transmitters.

The present paper, to our knowledge, is the first to demonstrate joint selection of the optimum input waveform bandwidth and load impedance based on load-pull data taken at multiple bandwidths. This will allow transmission that optimizes radar range detection, while allowing PAE and ACPR requirements to be met. It allows the maximum input signal bandwidth to be used under these given constraints.

To visualize the design approach, we introduce an extension of the Smith chart to include bandwidth of a linear frequency-modulation chirp waveform as the third dimension. We demonstrate the design optimization of Γ_L and the bandwidth of the chirp for all three design goals. To our knowledge, extension of the Smith chart has not been proposed for optimizations similar to this, although some evidence exists in the literature that the Smith chart has been extended for some other design purposes. Zolley describes the extension of a Smith chart into a sphere with two Smith charts stretched across its surface to represent and appropriately connect impedances with both positive and negative real parts. This approach overcomes limitations of conventional Smith charts in handling both types of impedances and is useful in the design of oscillators and active filters [9]. The theory of Zolley's spherical Smith chart is more completely laid out by Wu in terms of mapping rules and correlations between three- and two-dimensional coordinates [10]. Shamin *et al.* describe the generalization of the conventional Smith chart to include fractional circuit elements [11], and Kretzchmar and Shoonart describe a special Smith chart for lossy transmission lines [12].

II. THE SMITH TUBE

Figure 1 shows a conceptual drawing of the *Smith tube*. The horizontal cross-section of the tube is a Smith chart, and the vertical axis represents bandwidth. For each bandwidth value, the Smith chart represents the real and imaginary parts of the load reflection coefficient, Γ_L . Thus, the sought-for solution is within this tube: the combination of input chirp waveform bandwidth B and load reflection coefficient Γ_L that produces the desired Pareto optimization between the detection capabilities of the output waveform, the power-

added efficiency, and spectral compliance. If the center of the Smith tube's cross section represents an input waveform with zero bandwidth, then the upper half of the tube (positive values of bandwidth) represents the bandwidth of possible up-chirps, and the lower half represents the bandwidth values for possible down-chirps.

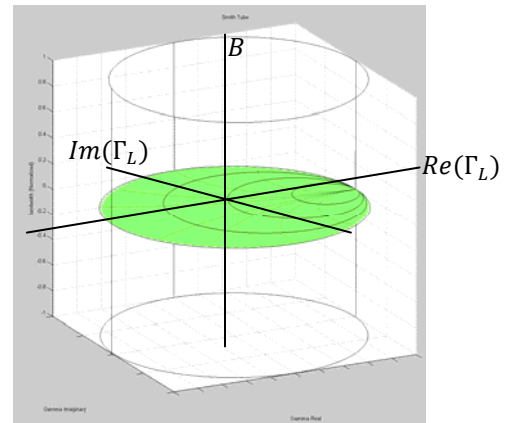


Fig. 1. The Smith tube. The vertical axis represents the bandwidth of the input chirp waveform, while the horizontal cross section of the tube is a conventional Smith chart.

III. OPTIMIZATION APPROACH

The values of PAE and ACPR representing the acceptable limits map to surfaces that can be plotted within the Smith tube. The following symbols are used here for compactness of notation: $\Gamma_r = Re(\Gamma_L)$ and $\Gamma_i = Im(\Gamma_L)$. Regarding the PAE, the surface of interest is the collection of all (Γ_r, Γ_i, B) combinations providing the minimum acceptable (worst acceptable) PAE value determined by design constraints. The ACPR surface of interest is the collection of all (Γ_r, Γ_i, B) combinations providing the maximum acceptable (worst acceptable) ACPR value determined by spectral constraints. Figure 2 shows a sample, conceptual plot of these surfaces within the Smith tube.

Typically, the PAE is based on power measurements from a broadband power sensor, and is only slightly dependent on input waveform bandwidth B . As such, the PAE surface of interest is expected to be nearly cylindrical, as shown in Fig. 2. However, for fixed designations of the channel of interest and the adjacent channel, the ACPR is expected to vary dramatically with input bandwidth B . For larger values of B , the spreading is wider, and fewer load impedances typically allow ACPR compliance. For larger values of B , more load impedances usually allow ACPR compliance. In many cases, if B is sufficiently small, any impedance on the Smith chart may provide an acceptable value of ACPR, while for large B there may not be any impedances providing acceptable ACPR. These concepts are expected to create PAE and ACPR surfaces of interest similar to those shown in Fig. 2.

The optimum design solution taken from the cylinder is the highest (or lowest if a down-chirp is desired) intersection point between the PAE and ACPR limiting surfaces. The

combination of $Re(\Gamma_L)$, $Im(\Gamma_L)$ and B mapping to this point should be used. This solution maximizes bandwidth (for range detection) while still providing PAE and ACPR values within the determined requirements.

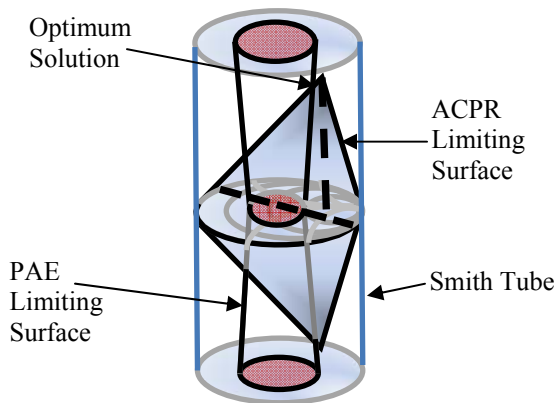


Fig. 2. Conceptual drawing of the Smith tube containing example surfaces for the limiting PAE and ACPR values. The optimum point is selected as the highest point of intersection (representing the largest bandwidth) between the surfaces representing the limiting PAE and ACPR values.

IV. MEASUREMENT RESULTS

Measurements were performed using a Skyworks amplifier on the nonlinear test bench at Baylor University. The laboratory setup is shown in Fig. 3. MATLAB is used to provide the waveform input to the signal generator. A Maury Microwave Automated Tuner System (ATS) was used to perform fundamental load-pull measurements (the laboratory currently does not possess harmonic tuning capabilities). The amplifier was excited at approximately 2-dB compression with a linear frequency-modulated (FM) chirp, and load-pull data was measured for a variety of bandwidth values between 1 MHz and 20 MHz. The goal is to find the combination of the load impedance and bandwidth that allows the largest bandwidth of the chirp while providing PAE and ACPR within the presented limitations.

For the design, limitations of $PAE = 7.0\%$ and $ACPR = -27.5$ dBc were specified (the PAE must be greater than or equal to 7.0 percent and the ACPR must be less than or equal to -27.5 dBc). To collect data needed for the design, load-pull measurements were performed for linear FM chirp excitations with the following bandwidths: 1, 5, 7.5, 10, 11.25, 11.875, 12.5, 13.125, 13.75, 14.325, 15, 15.625, 16.25, 17.5, and 20 MHz. The total RF input power was held constant for the entire experiment.

Figure 4 shows the optimum PAE and ACPR values for the Skyworks amplifier ascertained from load-pull measurements performed for chirps of different input bandwidth values. As expected, the PAE, while slightly increasing with bandwidth, holds relatively constant, while the minimum ACPR level rises as the input bandwidth is increased, rising dramatically as the third-order products begin to enter the defined adjacent channel, and then reaching a bit of a plateau. This follows intuitive expectation, as the

PAE measurement is performed with a broadband sensor, while the nonlinearity-induced amplifier spreading outside the band is directly related to the bandwidth of the input signal. The slight variation is observed over the bandwidth may be caused by the variation of the load impedance presented by the tuner over the chirp bandwidth, which was not taken into account. The plot of Fig. 4 indicates that, for the requirements given, the use of bandwidths above about 16 MHz will not be possible given the design constraints on PAE and ACPR: the best-case ACPR is larger than the allowed -27.5 dBc, and hence no termination in the Smith chart places the device within ACPR compliance.

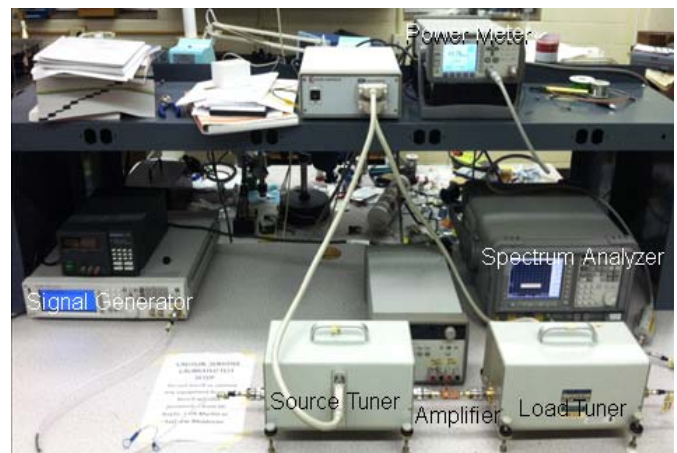


Fig. 3. Measurement setup

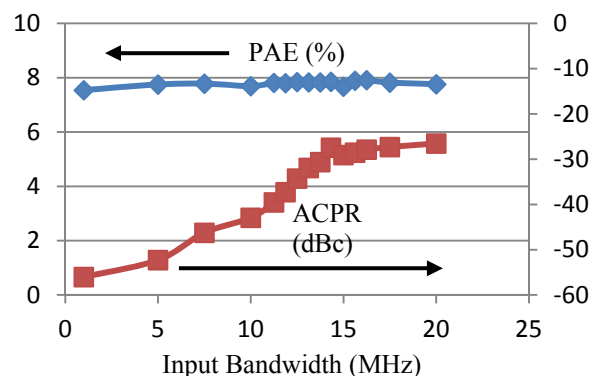


Fig. 4. Maximum power-added efficiency (PAE, left axis) and minimum adjacent-channel power ratio (ACPR, right axis) from measured load-pull results at different bandwidth values for the Skyworks amplifier

Figures 5 through 8 show specific load-pull data measured for some of these input bandwidth values: 12.5, 13.75, 15, and 20 MHz, respectively. The measured contours closest to the limiting values of $ACPR = -27.5$ dBc and $PAE = 7.0\%$ are shown, and the intersection of the acceptable regions ($ACPR < -27.5$ dBc and $PAE > 7.0\%$) are shaded. In Figures 5 and 6, it is seen that values of Γ_L providing both of these criteria exist for the bandwidths of 12.5 and 13.75 MHz. These “acceptable regions” of the Smith chart are shaded for clarity. For the 12.5 MHz chirp bandwidth (Fig. 5), the value

of Γ_L providing maximum PAE can actually be used, as it also provides acceptable ACPR. For the 13.75 MHz bandwidth, a true compromise must be performed between PAE and ACPR to get acceptable values of both.

For the load-pull measurements for the chirp bandwidths of 15 MHz and 20 MHz (Figures 7 and 8, respectively), no intersection of the ACPR and PAE criteria exist: no value of Γ_L on the Smith chart provides both ACPR < -27.5 dBc and PAE > 7.0 %.

Figure 9 shows the “Smith Tube” view of the measured data. A surface is shown consisting of the locus of points with the limiting ACPR value of -27.5 dBc. Also, the Γ_L values possessing PAE greater than or equal to 7.0 percent are shown for each of the measured bandwidths, giving an idea of the region of acceptable PAE values. The measured data point closest to the intersection point of the acceptable PAE and ACPR regions, which is optimal for design, was found to be $B = 13.75$ MHz, $\Gamma_L = 0.5377 \angle -21.65^\circ$. This point provides PAE = 7.57% and ACPR = -28.75 , both within the acceptable region. While the PAE and ACPR values indicate that higher bandwidth might be possible, the results are somewhat limited by the bandwidths at which load-pull data was taken. Vertical interpolation capabilities and measurements at a denser collection of bandwidths near the expected solution should provide a nearly exact result. However, this point is very near the boundary and demonstrates a useful result of this design approach. Figure 10 shows an artist’s rendering of how the PAE and ACPR surfaces appear in a picture more similar to Fig. 2.

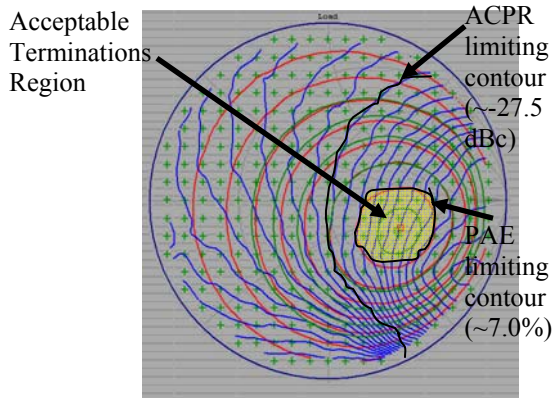


Fig. 5. Measured PAE (red) and ACPR (blue) load-pull contours for input waveform bandwidth of 12.5 MHz. The region of acceptable terminations meeting the PAE and ACPR requirements is shown.

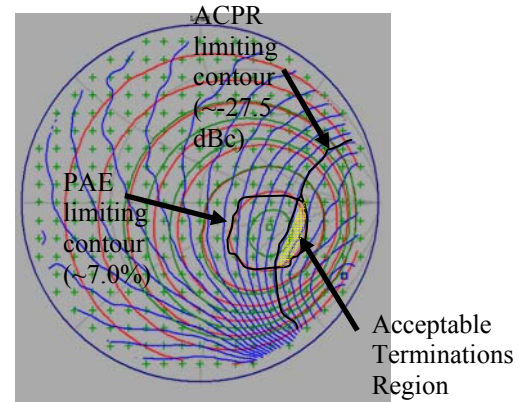


Fig. 6. Measured PAE (red) and ACPR (blue) load-pull contours for input waveform bandwidth of 13.75 MHz. The region of acceptable terminations meeting the PAE and ACPR requirements is shown.

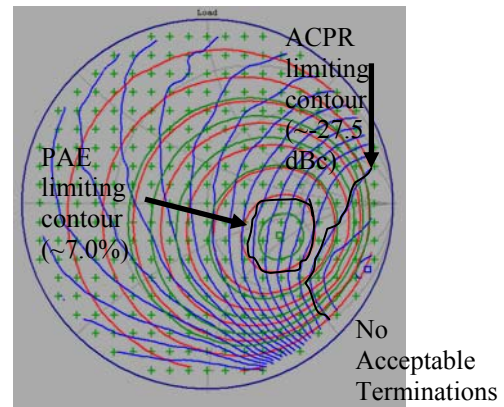


Fig. 7. PAE (red) and ACPR (blue) load-pull contours for input waveform bandwidth of 15 MHz. There is no region of acceptable terminations meeting both PAE and ACPR requirements.

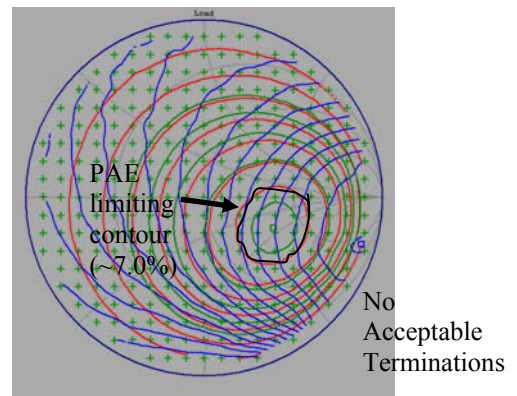


Fig. 8. PAE (red) and ACPR (blue) load-pull contours for input waveform bandwidth of 20 MHz. None of the terminations satisfy ACPR requirements, and there are no acceptable terminations for this design.

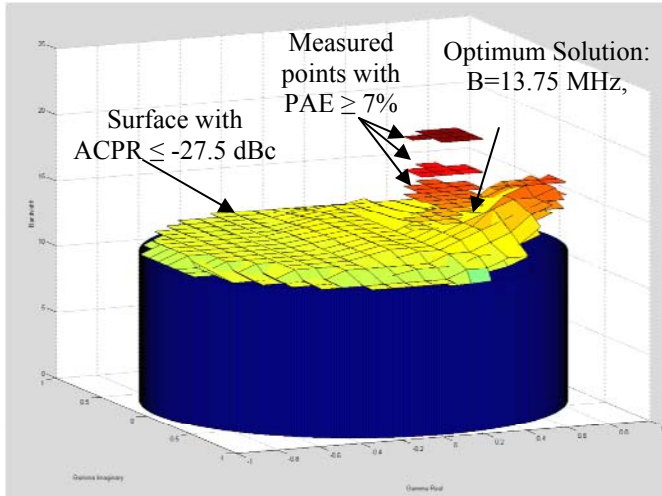


Fig. 9. Surfaces representing the locus of points shown in the Smith tube with ACPR = -27.5 dBc and PAE = 7.0%. The optimum solution is the highest intersection of the PAE and ACPR surfaces.

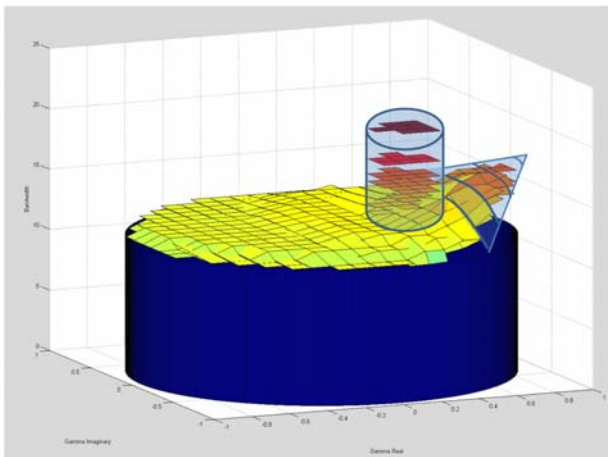


Fig. 10. Artist rendering of the cone and column using the data in Fig. 9. Compare to Fig. 2.

V. CONCLUSIONS

A design procedure has been presented to maximize the chirp waveform bandwidth of a radar transmitter while maintaining acceptable power-added efficiency and adjacent-channel power ratio. This design procedure will allow radar range detection capability to be maximized while still meeting spectral requirements and operating efficiently. The design approach utilizes load-pull data measured for multiple chirp waveform bandwidths, and the Smith tube is useful as a graphical method for choosing the optimum design combination of input waveform bandwidth and load reflection coefficient.

This work represents a significant step toward the joint circuit and waveform optimization of radar transmitter power amplifiers. A next step in developing the usefulness of this method is to design an intelligent search for the optimum

point within the Smith tube, which will make this design require a smaller number of measurement data points, and may facilitate real-time circuit optimization for future reconfigurable radars.

ACKNOWLEDGMENTS

The authors are grateful for the helpful insight and collaboration from Lawrence Cohen of the U.S. Naval Research Laboratory Radar Division. This work has been funded by a grant from the National Science Foundation (Award No. ECCS-1343316) to Baylor University.

REFERENCES

- [1] J. Martin, Master's Thesis: *Adaptive Load Impedance Optimization for Power Amplifiers in Reconfigurable Radar Transmitters*, Baylor University, 2012.
- [2] M. Fellows, C. Baylis, J. Martin, L. Cohen, and R.J. Marks II, "Direct Algorithm for the Pareto Load-Pull Optimization of Power-Added Efficiency and Adjacent-Channel Power Ratio," Accepted October 2013 for publication in *IET Radar, Sonar & Navigation*.
- [3] M. Fellows, C. Baylis, L. Cohen, and R.J. Marks II, "Radar Waveform Optimization to Minimize Spectral Spreading and Achieve Target Detection," 2013 Texas Symposium on Wireless and Microwave Circuits and Systems, Waco, Texas, April 2013.
- [4] M. Fellows, C. Baylis, L. Cohen, and R.J. Marks II, "Calculation of the Radar Ambiguity Function from Time-Domain Measurement Data for Real-Time, Amplifier-in-the-Loop Waveform Optimization," Automatic RF Techniques Group Conference, Columbus, Ohio, December 2013.
- [5] J. Sevic, K. Burger, and M. Steer, "A Novel Envelope-Termination Load-Pull Method for ACPR Optimization of RF/Microwave Power Amplifiers," 1998 IEEE MTT-S International Microwave Symposium Digest, June 1998, Vol. 2, pp. 723-726.
- [6] J. Sevic, "Large Signal Automated Load-Pull Characterization of Adjacent-Channel Power Ratio for Digital Wireless Communication Systems," 1996 IEEE MTT-S International Microwave Symposium Digest, June 1996, pp. 763-766.
- [7] Q. Wu, H. Xiao, and F. Li, "Linear Power Amplifier Design for CDMA Signals: A Spectrum Analysis Approach," *Microwave Journal*, 1998.
- [8] F.N. Sechi, "Design Procedure for High-Efficiency Linear Microwave Power Amplifiers," *IEEE Transactions on Microwave Theory and Techniques*, Vol. 28, Pt. 1, November 1980, pp. 1157-1163.
- [9] C. Zelle, "A Spherical Representation of the Smith Chart," *IEEE Microwave Magazine*, Vol. 8, Issue 3, June 2007, pp. 60-66.
- [10] Y. Wu, Y. Zhang, Y. Liu, and H. Huang, "Theory of the Spherical Generalized Smith Chart," *Microwave and Optical Technology Letters*, Vol. 51, Issue 1, November 2008, pp. 95-97.
- [11] A. Shamin, A.G. Radwan, and K.N. Salama, "Fractional Smith Chart Theory," *IEEE Microwave and Wireless Components Letters*, Vol. 21, No. 3, March 2011, pp. 117-119.
- [12] J. Kretzschmar and D. Schoonaert, "Smith Charts for Lossy Transmission Lines," *Proceedings of the IEEE*, Vol. 57, No. 9, September 1969, pp. 1658-1660.